THE JOURNAL OF PHYSICAL CHEMISTRY B

Article

pubs.acs.org/JPCB

Decomposition of Lignin from Sugar Cane Bagasse during Ozonation Process Monitored by Optical and Mass Spectrometries

J. A. Souza-Corrêa,[†] M. A. Ridenti,[†,‡] C. Oliveira,[†] S. R. Araújo,[§] and J. Amorim*[,†,‡]

[†]Laboratório Nacional de Ciência e Tecnologia do Bioetanol − CTBE/CNPEM, 13083-970, Campinas, São Paulo, Brazil

[‡]Instituto de Física Gleb Wataghin, Universidade Estadual de Campinas − UNICAMP, 13083-859, Campinas, São Paulo, Brazil

[§]Laboratório Nacional de Nanotecnologia − LNNANO/LME/CNPEM, Rua Giuseppe Máximo Scolfaro, 10.000, Polo II de Alta Tecnologia, 13083-100, Campinas, São Paulo, Brazil

ABSTRACT: Mass spectrometry was used to monitor neutral chemical species from sugar cane bagasse that could volatilize during the bagasse ozonation process. Lignin fragments and some radicals liberated by direct ozone reaction with the biomass structure were detected. Ozone density was monitored during the ozonation by optical absorption spectroscopy. The optical results indicated that the ozone interaction with the bagasse material was better for bagasse particle sizes less than or equal to 0.5 mm. Both techniques have shown that the best condition for the ozone diffusion in the bagasse was at 50% of its moisture content. In addition, Fourier transform infrared spectroscopy (FTIR) and scanning electron microscopy (SEM) were employed to analyze the lignin bond disruptions and morphology changes of the bagasse surface that occurred due to the ozonolysis reactions as well. Appropriate chemical characterization of the lignin content in bagasse before and after its ozonation was also carried out.

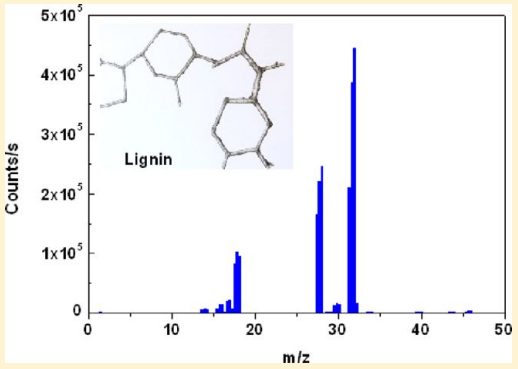

INTRODUCTION

Global warming and the reduction of fossil carbon reserves have led to the progressive introduction of biomass as a renewable source of carbon. A successful example on this issue is the large scale use of sugar cane ethanol in Brazil to power light Flex vehicles with fuel engines that can run on any mixture of gasoline and ethanol. To optimize bioethanol production, high-yield methods to obtain fermentable sugars from lignocellulosic biomass are needed.

The ordinary source of these fermentable sugars in lignocellulosic materials is the cellulose component of cell wall plants, which is composed by glucose chains. To access these cellulosic structures, it is necessary to take out two other components from the cell wall: hemicellulose and lignin. The lignin is the main constitutive that could strongly disturb the bioprocess in order to obtain bioethanol. However, by considering the concept of a biorefinery, additionally to the biofuels other chemical products could be aggregated in order to make the whole process economically viable. For example, chemocatalytic works are currently being developed for valorizing lignin in this sense.[1]

Lignin represents about 10% to 30% of the biomass present in the world. It can be characterized as an amorphous and complex three-dimensional polyphenolic polymer composed by a set of one or more methyl and hydroxyl groups attached to aromatic rings, with antioxidant properties. Typically lignin permeates the matrix of cellulose fibers and fills the interstices between cellulose, hemicellulose, and pectin components, acting as a "link" between these structural components of the biomass cell wall. Several pretreatment methods have been proposed to fragment lignocellulosic arrangements.[2−4] Specific reactive chemical species such as ozone and molecular oxygen have an important role in the deconstruction of lignin matrix.[5−14]

Ozone is a nonlinear triatomic molecule with an obtuse bond angle and two oxygen−oxygen bonds of equal length.[15] Ozone has been used on biomass treatments because it has the property of cleavage carbon−carbon double and triple bonds efficiently and eventually single bonds. Due to this characteristic, lignin degrades rapidly to low molecular weight compounds when it is in contact with ozone while polysaccharides were much more resistant.[8−14] The ozone attacks lignin selectively (if compared to carbohydrate) and is more evident when hydroxyl and hydroperoxyl radicals are reduced in the medium.[16] It was also remarked that extensive ozonation of lignin manly attacked the aromatic structures, preserving, mostly unbroken, the side chains attached onto these aromatic rings.[8,17]

Criegee's mechanism for oxidative cleavage of carbon−carbon double bonds (the so-called ozonolysis process) predicts that the ozonation reactions over alkene compounds (C═C) proceeds in three different steps.[15,18] The ozone reacts with the alkenes via 1,3-dipolar cycloaddition to form the 1,2,3-trioxolane intermediate (first ozonoide) (see Figure 1a). The

Received: December 11, 2012
Revised: January 26, 2013
Published: February 26, 2013

dx.doi.org/10.1021/jp3121879 | J. Phys. Chem. B 2013, 117, 3110−3119

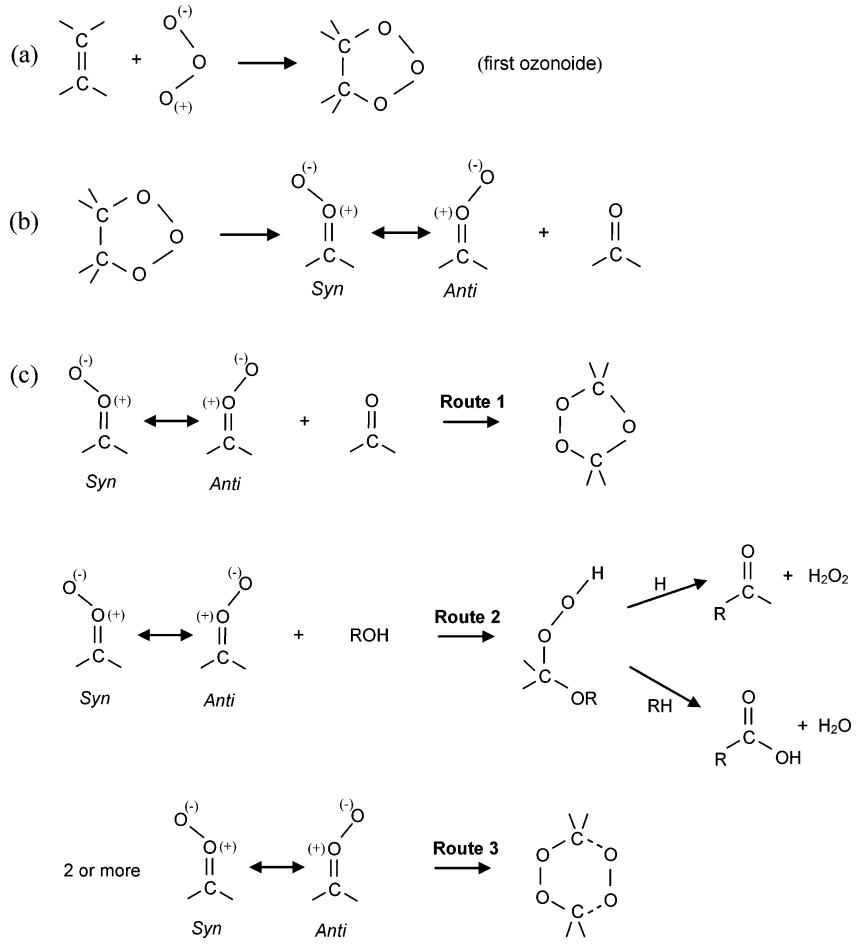

Figure 1. Criegee's mechanism routes (adapted from ref 18).

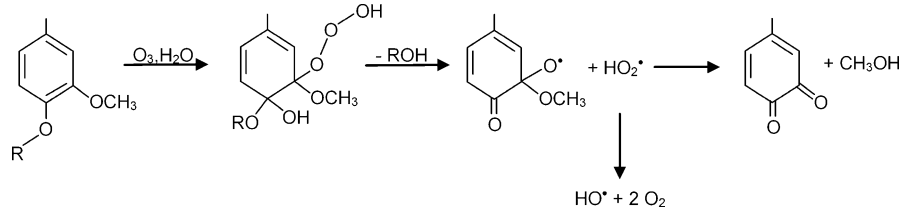

Figure 2. Reaction mechanism for the formation of hydroxyl radical on ozone treatment of an aromatic lignin unit.[17]

decomposition of the first ozonoide via 1,3-dipolar cycloreversion yields the *syn* and *anti* isomers of "zwitterions" (the so-called carbonyl oxide) and a carbonyl compound (see Figure 1b). Depending on the reaction conditions, three different routes could be followed[18] (see Figure 1c): route 1 - a final ozonoide can be produced by one more 1,3-dipolar cycloaddition in which a carbonyl oxide and a carbonyl compound recombine; route 2 - carbonyl oxide may react with a solvent (e.g., H_2O) to form a hydroperoxide intermediate, which may generate another carbonyl compound (liberating H_2O_2) or an organic peroxide (liberating H_2O); and route 3 - dimerization or polymerization of "carbonyl oxide" may occur to form diperoxides or polymeric peroxides. Figure 1a–c depicts the Criegee mechanism with the possible routes.

The mechanism of interaction between ozone and lignin remains not fully understood.[19] As mentioned above, ozone initially reacts with carbon double bonds in the macromolecules breaking the aromatic ring structure or the aliphatic bonds,[18] although it could promote the cleavage of the β-O-4 bonds as well.[8,19] Other reactions are also possible, such as the hydroxylation of the aromatic rings of the coniferylic or paracoumarylic structures of lignin or the oxidative cleavage of the methoxyl groups.[19] The reactions with carbon double bonds and the β-O-4 bonds in the macromolecules are believed to be fast, explaining the initial high rates of ozone consumption and lignin degradation observed by Binder et al.[9] and Mbachu and Manley.[10] Ozone could also cleavage the carbon–carbon bonds of aromatic rings, but usually at a slower rate than observed for alkene substrates.[20,21] Figure 2 shows an example of reaction mechanism products on ozone treatment of an aromatic lignin unit.

After the formation of hydroxyl radical, the resultant cathecol may be oxidized by ozone leading to low weight fragments, such as HCOOH (see Figure 3).

The specific routes of the ozonolysis process could justify the appearance of some chemical species in the mass spectra. Many chemical species came from reaction products related to lignocellulosic material decomposition during the ozone attack.

dx.doi.org/10.1021/jp3121879 | J. Phys. Chem. B 2013, 117, 3110–3119

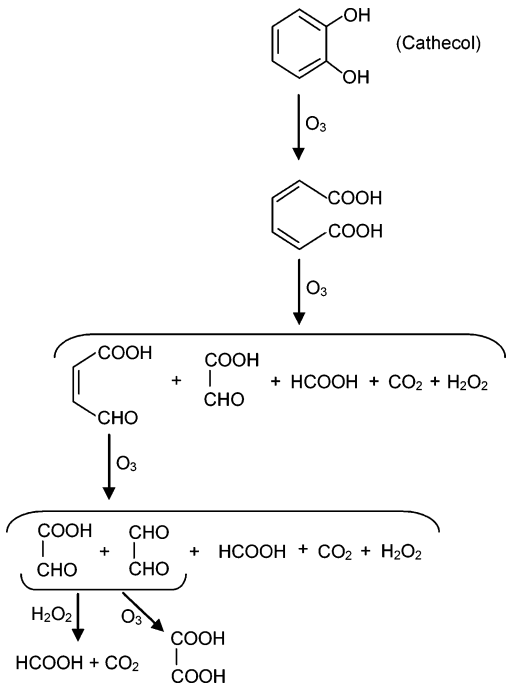

Figure 3. Cathecol oxidation by ozone leading to low weight fragments.[17]

The most important products are carboxylic acids, such as formic acid, acetic acid, oxalic acid, and other dicarboxylic acids.[8,16] Moreover, many radicals could be formed in indirect reactions between ozone and lignin, such as OH, H_2O, H_2O_2 and O_2.[8,17,22]

Several techniques have been applied to better understand the lignin decomposition.[1,9,10,13,23−27] For example, mass spectrometry has been employed for lignin investigations.[23−27] The time-of-flight secondary ion mass spectrometry (ToF-SIMS) was extensively used to investigate the characteristic of lignin fragments, which were mostly based on guaiacyl and syrigil rings, by showing that ToF-SIMS is a useful tool for lignin structural analysis.[23−25,27] Some optical analyses have been used to evaluate the effect of ozone on biomass as well, in particular on its lignin structure.[9,10,13]

In this work, an alternative mass spectrometry technique based on an electrostatic quadrupole spectrometer for molecular beam mass/energy spectrum analysis was used to investigate the volatile species emitted from the interaction of ozone molecules with the lignin content on sugar cane bagasse in order to understand the mechanisms of ozone reaction over C−C, C−O, and C−H bonds of these lignin structures as a function of treatment time and moisture. Many radicals detected have indicated strong correlation between ozone attack and the lignin bagasse degradation according to Criegee's mechanism. Moreover, ozone concentrations were monitored in real time during the bagasse ozonation by using optical absorption spectroscopy for various ozonation conditions. Other complementary analyses were also employed, such as SEM and FTIR techniques. The chemical content of lignin in bagasse before and after the ozonolysis process was evaluated.

MATERIALS AND METHODS

The basic configuration of pretreatment setup considering the analytical techniques employed during the ozonation of bagasse samples, such as optical spectroscopy and mass spectrometry, are depicted in Figure 4.

Ozonation on Bagasse Material. A sinusoidal wave function generator (Minipa 20 MHz model MFG 4221) was used as a source of an ozonizer based on atmospheric pressure dielectric barrier discharge (DBD) plasmas. The generator was connected to an amplifier, which in turn was linked to a high-voltage (HV) transformer in series with a 20 kΩ resistor. The generator signal at a fix voltage (5 V) was amplified until the voltage over the DBD electrodes has achieved about 13.0 kV. This DBD power supply was set at 10.0 kHz and connected into three DBD devices, each composed by coaxial electrodes

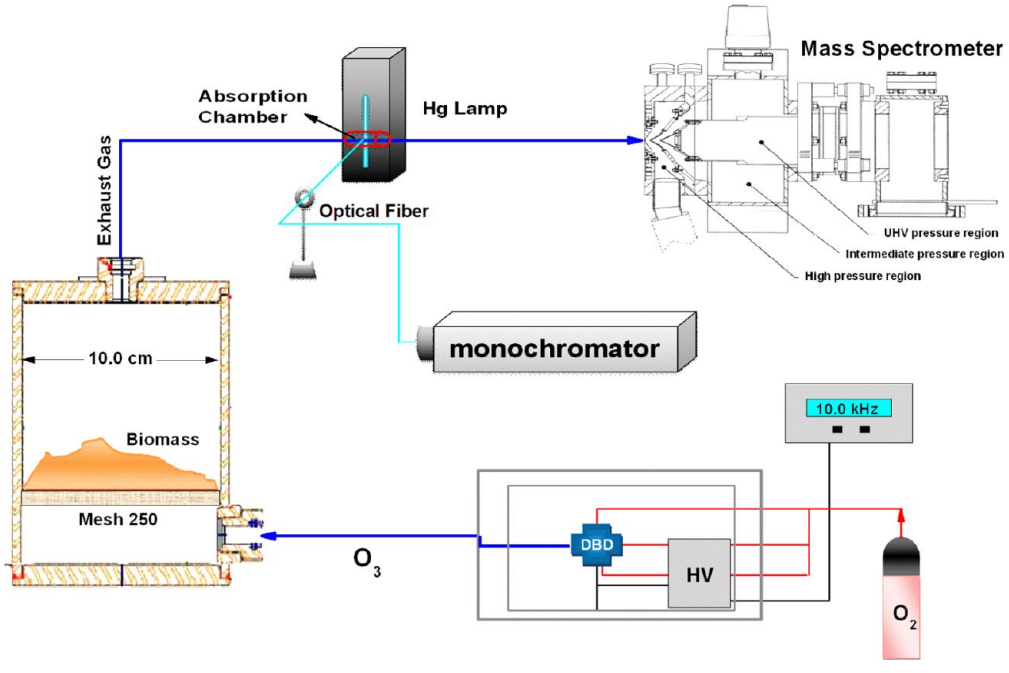

Figure 4. Experimental setup considering the analytical techniques employed during the ozonation of bagasse samples.

dx.doi.org/10.1021/jp3121879 | J. Phys. Chem. B 2013, 117, 3110−3119

separated by a dielectric ceramic tube. The DBD apparatus was in a cross array (see Figure 4). The system was fed by 0.3 SLM of oxygen (99.8% purity (impurity composition: H_2O < 200.0 ppm; CO < 10.0 ppm; NH_3 < 25.0; SO_2 < 5.0 ppm; NO_x < 2.5 ppm; H_2S < 1.0 ppm. The amounts of impurity are despicable. No hydrocarbon compounds were present in our feed gas.)) on each device (total of 0.9 SLM).

The ozonation process was carried out at room temperature to treat 20.0 g of dry integral sugar cane bagasse samples (contents of fibers, parenchyma and epidermis). Our experiments were performed by changing the moisture quantity on the bagasse (10%, 25%, 50% and 75% of H_2O added in biomass samples) by fixing the typical particle size of milled bagasse at 0.5 mm. The wetness contents in bagasse were measured by using an analytical moisture balance (Sartorius MA35). Another set of experiments was executed by varying the bagasse size (0.08 mm, 0.2 mm, 0.5 mm, 1.0 mm and 2.0 mm) with fixed moisture content in bagasse at 50%. The particle sizes of bagasse samples were adjusted by using a variable speed rotor mill (Fritsch model Pulverisette-14). Each amount of bagasse for the different conditions was placed into a stainless steel reactor (10 cm inner diameter; 12.0 cm height) on a wire disk (250 μm mesh size; see Figure 4). The basic reactions related to ozone and oxygen species that may occur at the DBD device feed by O_2 gas are

$$O_2 + O + M \rightarrow O_3 + M \quad \text{(three body reaction)} \tag{1}$$

$$O_3 + \text{UV photon} \rightarrow O_2 + O \tag{2}$$

$$O_3 + O \rightarrow 2O_2 \tag{3}$$

$$2O \rightarrow O_2 \tag{4}$$

Therefore our plasma has mainly produced O_2 and O_3 species.

Mass Spectrometry. The mass spectrometry (MS) analysis was conducted on a molecular beam mass spectrum (MBMS) Hiden HPR60−500 spectrometer in order to assess neutral chemical species from sugar cane bagasse that could be volatilized during 4 h of bagasse ozonation process based on DBD plasmas (Figure 4). The residual gas analysis (RGA) mode was used to record spectra of neutral species up to m/z = 500, with a step resolution of 0.3. Before the measurements of neutral species, the tuning of the system parameters were made in order to optimize the detection of neutrals (RGA map tune mode). The ionization process of neutral species occurred inside the mass analyzer from the filament emission source with ionizing electron energy of 70 eV. More technical details about the characteristics of the HPR60 can be obtained in the Hiden Analytical Manual.[28]

Optical Absorption Spectroscopy. Experiments were also carried out by using optical absorption spectroscopy (OAS) in order to access the behavior of ozone concentration as a function of treatment time by changing moisture contents in the bagasse, as well as for several particle size of milled bagasse by monitoring in real time the exhaust gas from the treatment reactor. Ozone concentrations were determined during the bagasse treatment by spectroscopic technique, employing the Beer−Lambert's Law. In this sense, an optical fiber was connected to the entrance slit of a monochromator (0.55m focal length and 1800 lines/mm grating) and placed perpendicular to a quartz absorption cell (0.8 cm inner diameter), see Figure 4. The experiments were carried out by monitoring for 3 h the absorption of ozone molecules on the Hg emission line at 253.65 nm.[29] The detector used to record the spectra was a Synapse CCD 2056 × 512 pixels.

Scanning Electron Microscopy. Scanning electron microscopy (SEM) was used to analyze the morphology of the bagasse surface before (raw bagasse) and after the ozonation pretreatment. In this work, an FEI Inspect F50 High-Resolution SEM was employed in order to obtain the images.

Fourier Transform Infrared. Fourier transform infrared technique (FTIR) was applied to obtain the IR spectra of lignin bagasse content before (raw bagasse) and after the ozonation pretreatment by using a Perkin-Elmer Spectrum 400 spectrometer for mid- and near-IR regions (4000−400 cm^{-1}) with resolution of 0.5 cm^{-1} in order to perform the measurements.

Physicochemical Lignin Analyses. The bagasse samples before and after several ozonation process and conditions were chemically characterized in order to determine their lignin contents (soluble and insoluble). The chemical analytical methodology used was developed by Rocha et al. and validated by Gouveia et al.[30,31]

RESULTS AND DISCUSSION

Before treating the bagasse samples, the whole system was operated for 1 h on empty reactor conditions (i.e., without biomass inside it) in order to obtain the residual mass spectra of the system. This so-called "control spectrum" was obtained by a mean of 20 mass scan cycles (Figure 5). From Figure 5, it could be noted that there were mass detections between m/z = 0 and m/z = 50, while masses greater than m/z = 100 were not detected.

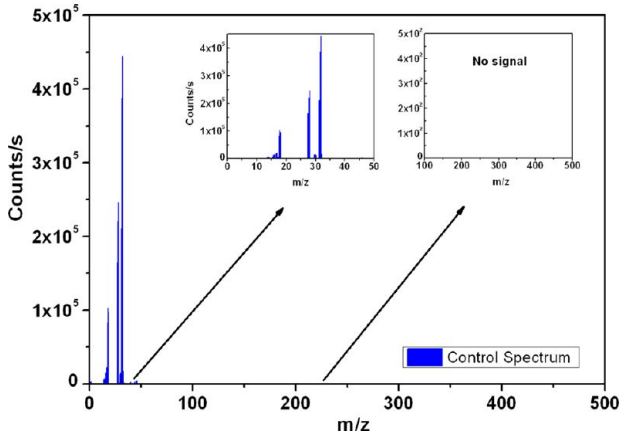

Figure 5. Mass control spectrum up to m/z = 500.

The gas mixture resulting from the bagasse ozonation process was directly conducted from the reactor exit into the mass spectrometer entrance in order to facilitate chemical species detection. Continuous scans were done during the bagasse ozonation to obtain spectra similar to those shown in Figure 5. No heavy mass ($\geq m/z$ = 100) was detected on the spectra of the ozonation process as well. The sample treatment lasted 4 h for each moisture condition on the bagasse. After the mass scan, the background subtract mode were used in order to remove the data related to the control spectrum from that obtained through the biomass treatment. Proceeding in this way, the spectra analyzed have contained only chemical species desorbed by the biomass, and no contributions from the

dx.doi.org/10.1021/jp3121879 | J. Phys. Chem. B 2013, 117, 3110−3119

system, e.g., reactor wall, were involved. A sequence of mass spectra from biomass as a function of time (only five temporal samples) is shown in Figure 6. Essentially, the differences

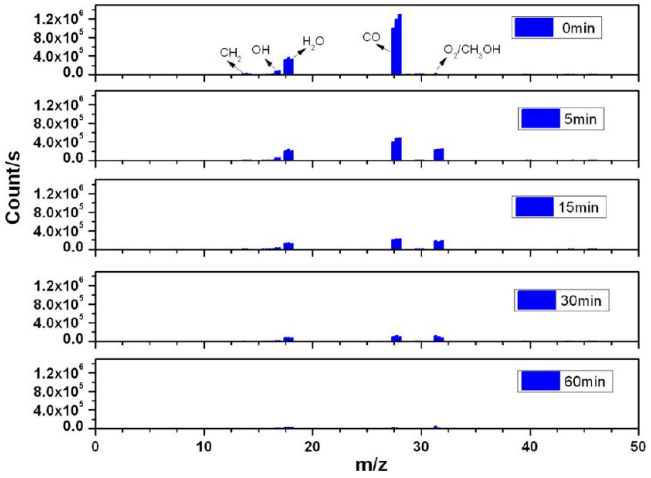

Figure 6. Mass spectra of bagasse (50% moisture; 0.5 mm size) as a function of ozonation time after control spectrum subtraction. Some species are indentified for visible peaks in the mass spectrum according to the count/s scale range.

observed were in the counting intensity for each ozonation time for each species. Figures 7, 8, and 9 show the peak measurements done on the bagasse mass spectra for each species after the subtraction of the control spectrum.

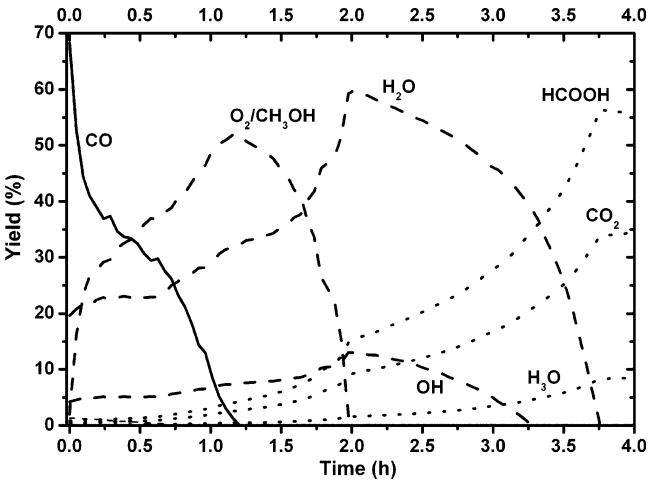

Figure 7. Species yield (%) as a function of bagasse ozonation treatment time (moisture of 50%).

Mass spectra are employed in this work in order to probe volatile species during the attack of ozone on bagasse samples as a function of moisture and treatment time to evaluate the interaction of ozone with the lignocellulosic material.

In Figure 7 the yields of radicals as a function of time can be seen. For the present results, we used yields of specific masses (relative contribution to the total signal) instead of counts per second obtained directly from the MBMS to show the relative importance of each species. It should be mentioned that the species appearing in Figure 7 are the most abundant. Others species with less count rates, i.e., faint yields, may be important

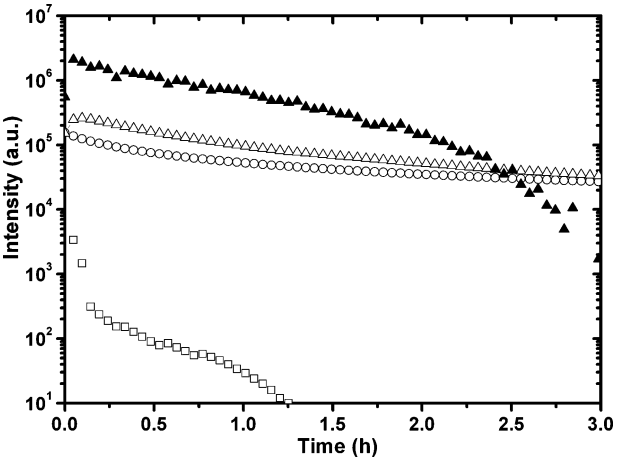

Figure 8. Concentrations of O_2/CH_3OH densities as a function of time according to the moisture amount on the bagasse. Humidity of 10% (open circles), 25% (open triangles), 50% (filled triangles), and 75% (open squares).

due to its reactivity but will not be subject of the present study. The relative yield Y_i^r of a given mass was calculated as

$$Y_i^r(\%) = \frac{Y_i^a}{\sum_i Y_i^a} \times 100 \quad (5)$$

where, Y_i^a is the absolute count rate of a given mass *i*. The count due to specific species was divided by the sum of counts for all recorded masses (m/z = 1−100).

From Figure 7 it can be also noted that CO is the first radical formed when the treatment is launched. The production almost instantaneously is in good agreement with the reaction scheme proposed by Criegee[18] (see Figure 1). It disappears after around 1 h and 15 min of treatment. The breaking of C═C bonds is the origin of high rate of CO production in the first instant of the treatment. This result clearly shows the accuracy of Criegee's model to explain the ozonation of lignin and corroborates the interpretation of oxidation of β-O-4 bonds. Important intermediary states such as O_2, CH_3OH, OH, and H_2O formed as a result of the cleavage of aromatic rings (see Figure 2 and Figure 3), which is a slow reaction. Further experiments should be done to discriminate O_2 and CH_3OH since they have the same mass (m/z = 32). Moreover, by using the MS technique it is not possible to discriminate which amount of H_2O detected by the equipment were directly related to the Criegee's reactions and which came from the moisture in the bagasse samples. In this sense, other experiments should be carried out in order to clarify this aspect as well. In the third phase, HCOOH, CO_2 and H_3O radicals are formed. The formation of this radicals is due to oxidation of the cathecol, which is a secondary process and explains why these species appear lately in the treatment (see Figure 3). These are important results to validate the reaction paths during the interaction of ozone with the biomass.

Schultz-Jensen et al. have demonstrated that the amount of water in the biomass (wheat straw in their case) during the ozonation process was fundamental in order to achieve a good efficiency on the lignin degradation.[13,14] In this sense, we evaluated the variation of water amount as a function of bagasse ozonation time for the different moisture conditions (Figure 8).

We choose to monitor O_2/CH_3OH molecules desorbed by the bagasse since they are key species in the Criegge's kinetic

dx.doi.org/10.1021/jp3121879 | J. Phys. Chem. B 2013, 117, 3110−3119

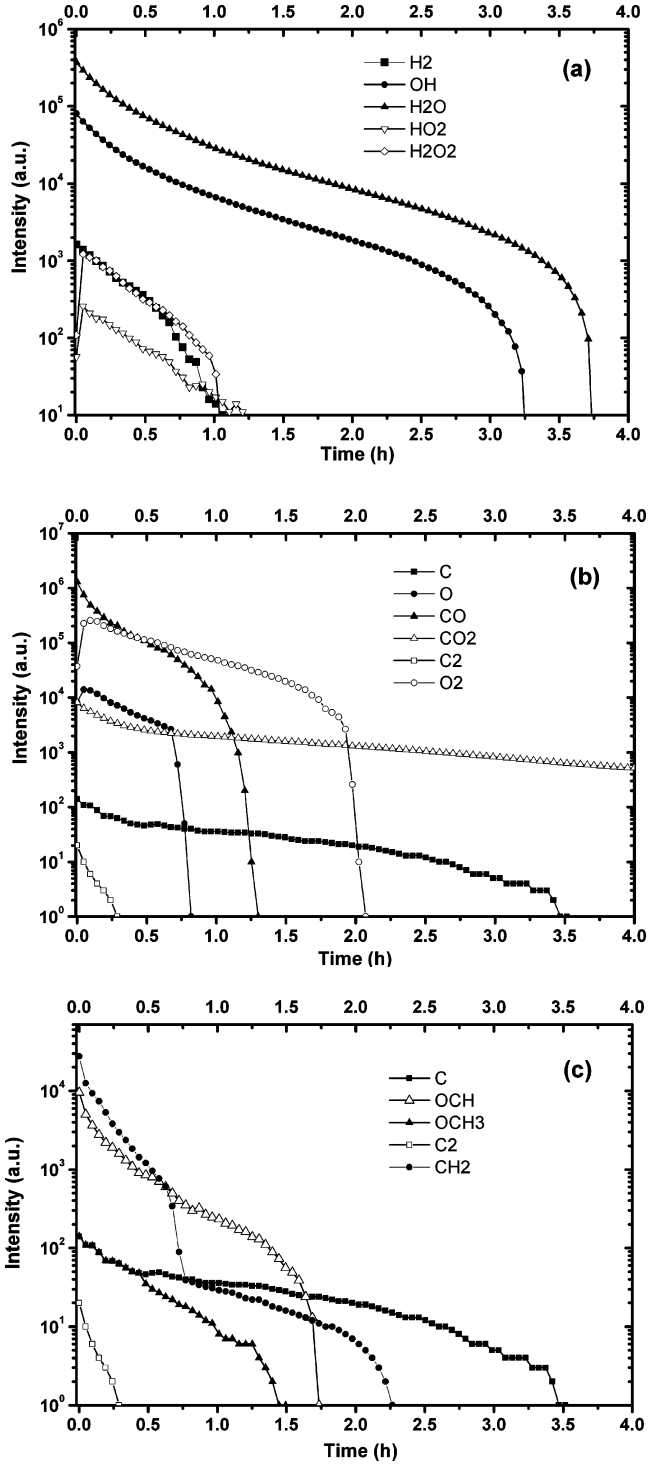

Figure 9. Mass concentration for different chemical species as a function of time detected during the ozonation process of sugar cane bagasse (size: 0.5 mm; moisture: 50%) for (a) H_2, OH, H_2O, HO_2, and H_2O_2; (b) C, O, CO, CO_2, C_2, and O_2; (c) C, OCH, OCH_3, C_2, and CH_2.

scheme, as can be seen in Figure 2. One could see that the bagasse with 10% of humidity (minimum amount of water content in dry bagasse condition), the O_2/CH_3OH densities slightly decrease as a function of time. As the moisture amount was increased in the bagasse to 25%, the density slightly increased because more ozone is absorbed in the bagasse, giving origin to the break of lignocellulosic chains. Note that the count intensity is almost the same in these last two cases. The best condition was when the humidity was increased to 50% where the O_2/CH_3OH densities attained the highest level, around 1 order of magnitude higher than 10% and 25% cases. Otherwise, when the amount of water was further increased to 75% in the bagasse, the O_2/CH_3OH densities presented the lowest value due to the low probability of absorption of this specie on the biomass, in this case, around 4 orders of magnitude lower than the 50% condition. This result indicates that the H_2O amount in the biomass should allow a better interaction/diffusion of the ozone in the lignocellulosic structure, as was verified by Schultz-Jensen and collaborators.[13,14]

Figure 9a–c presents the counting intensities as a function of time for each specific chemical species detected in the spectra for the case of sugar cane bagasse with 50% of moisture. Similar spectra were obtained for the other moisture cases, although they are not shown herein. Figure 9a shows the measurements for H_2, OH, H_2O, H_2O_2, and HO_2, which are typical radical products of direct ozone reactions with alkenes and aromatic rings. The most important species are OH and H_2O due to their large abundance, lasting more than 3 h in the reactor. It can be seen that until 1 h of treatment, the occurring reactions have also released H_2, HO_2, and H_2O_2, which disappeared after that time.

Figure 9b shows the measurements of C, O, CO, C_2, and O_2 which would be better correlated with fragments of the lignin itself. Within 0.25 h of treatment, the C_2 was exhausted completely. The CO was detected until 1.75 h and O about 0.75 h. The CO_2 is the unique species that was detected more than 4 h of treatment. It can be remarked that high concentration of C atoms is observed until 3.5 h of treatment, indicating the action of ozone in the deconstruction of the lignocellulosic sample.

Figure 9c shows that within 1.5 h of treatment, the releasing of OCH_3 occurred. The presence of an OCH radical can also be seen. Further experiments should be done to evaluate whether this resulted from the breaking the OCH_3 in the mass spectrometer ionization chamber or if it came from the process itself. OCH_3 is present in the monolignols as conyferyl and synapil alcohols, which are model compounds of lignin (guayacil and syringil units, respectively). The breaking of this radical bond to the phenol structure is revealed here, and certainly is a very important result. CH_2 and C radicals are long-lived along the treatment, and their release is an indication of the breakdown of lignocellulosic structure.

The effect on the physicochemical properties of lignin as a function of ozonation time is shown in Table 1. From Table 1 it was observed that the lignin has reduced its content in comparison with the raw bagasse as the ozonation time has increased. At 4 h of pretreatment, ~65% of delignification was achieved, indicating a good efficiency in the process. This result is in accordance to that of Schultz-Jensen et al., who indicated

Table 1. Lignin contents in bagasse before and after the ozonation process. The zero time corresponds to the raw material lignin contents without treatment

time (h)	lignin (%)
0	38.5 ± 0.2
1	18.1 ± 0.2
2	15.7 ± 0.9
4	13.6 ± 0.6

dx.doi.org/10.1021/jp3121879 | J. Phys. Chem. B 2013, 117, 3110–3119

delignification efficiencies on wheat straw material from 50% to 95% for ozone treatment occurring between 1 h and 7 h, respectively.[13]

For the experiments carried out by OAS, ozone density were measured as a function of time for different moisture contents in bagasse as well as for several bagasse particle size configurations (see Figure 10a,b, respectively). It is important

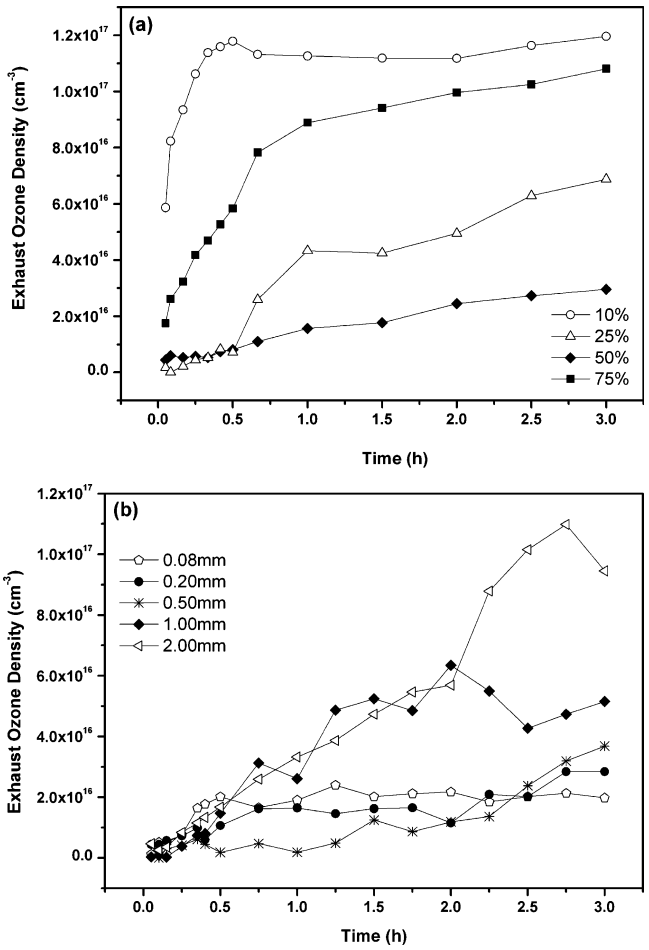

Figure 10. Ozone density exhausted from the reactor exit as a function of time for (a) different moisture contents in bagasse at 0.5 mm of typical particle size and (b) for several bagasse particle sizes at 50% moisture content.

to note that the measurements in Figure 10 correspond to the exhausted ozone density from the reactor exit, indicating that high concentration means less absorption has occurred. From Figure 10a, it was confirmed for the samples with different humidity content in bagasse (10%, 25%, 50%, and 75%) and fixed particle size at 0.5 mm that the efficiency of ozone absorption on bagasse surface increased as the amount of moisture in bagasse was improved up to 50%. After that amount, for example at 75%, it was observed that the efficiency in absorption was reduced, being worse than the 25% case. This result is in agreement with Figure 8 based on mass spectrometry, indicating the consistency of both analytical methods applied.

From Figure 10b, for a fixed moisture content in bagasse at 50% by varying the particle size of milled bagasse (0.08 mm, 0.2 mm, 0.5 mm, 1.0 mm and 2.0 mm), it was observed that up to 30 min of treatment there was no influence of bagasse size on the ozone interaction with the bagasse surface. From this time on, it was possible to see that typical sizes equal to or below 0.5 mm had a better absorption of ozone in comparison with greater particle sizes (1.0 mm and 2.0 mm), although it was not so conclusive which size really best improved the ozonation process. There was an indication that during 40 min and 90 min, the case of 0.5 mm had a small improvement if compared to the 0.08 mm and 0.2 mm configuration.

The IR spectra of the bagasse before and after the ozonolysis are shown in Figure 11. The FTIR spectrum showed significant

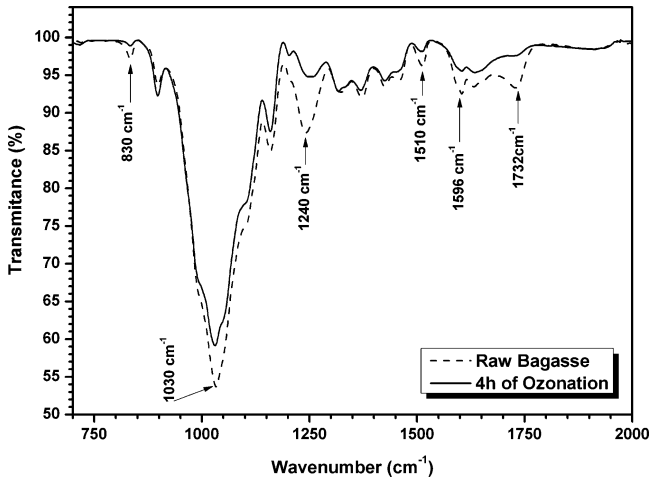

Figure 11. FTIR spectra of both raw bagasse and a bagasse sample treated by ozone for 4 h. Different bands related to lignin structure were detected.

variations in the range between 750 cm^{-1} and 2000 cm^{-1}. It was possible to note that many structures in the IR spectrum for the sample treated for 4 h reduced or changed its shape for specific wavenumbers in relation to the raw material signature, indicating a strong interaction between ozone and lignin bonds.

As can be seen in Figure 11, the main changes were in the bands 830 cm^{-1}, 1030 cm^{-1}, 1240 cm^{-1}, 1510 cm^{-1}, 1596 cm^{-1}, and 1732 cm^{-1}. Absorption bands located in the region 1765−1615 cm^{-1} are the result of vibrations of carbonyl groups.[32] Aromatic skeletal vibrations and C═O stretching are found in the region 1600−1500 cm^{-1}.[33] It can be seen in Figure 11 that at 1596 cm^{-1} this functional group is present in the spectrum, which is related to a very strong aromatic ring stretch and C═O stretch.[34] The 1510 cm^{-1} absorption band is known as a trace to identify the presence of lignin in the pulp. It is due to vibrations of the phenyl-ring skeletal of lignin macromolecules. It can also be used as a probe to monitor the lignin core degradation during a given process. Recently, Yu,[35] using synchrotron FTIR microspectroscopy, identified lignin in the 4000−800 cm^{-1} wavenumber range and could show that the lignin concentration and distribution can be monitored by measuring the area under the peak at 1510 cm^{-1}.

The region 1500−1400 cm^{-1} is characterized by C−H asymmetric deformation in −OCH_3 and CH_2 symmetric scissoring in pyran ring.[34,36,37] Interpretation of the spectra in the 1400−1300 cm^{-1} wavenumber region shows that many C−H and O−H deformations take place. Others species such as CH_3, CH_2, and phenolic OH are also present.[34]

The most prominent bands of the lignin spectra are in the region 1300−1000 cm^{-1}. The absorption band between 1240 and 1210 cm^{-1} allows one to probe the asymmetric stretching

dx.doi.org/10.1021/jp3121879 | J. Phys. Chem. B 2013, 117, 3110−3119

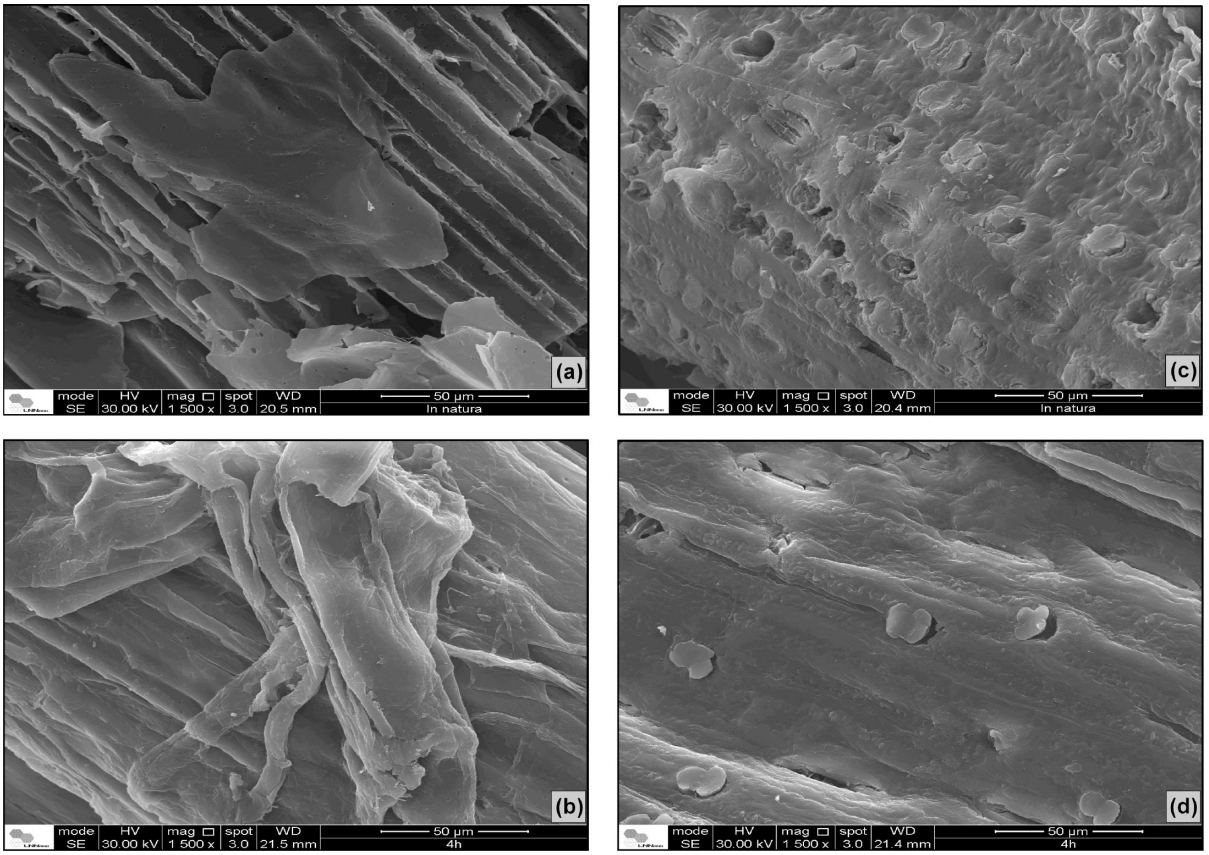

Figure 12. SEM images for (a) raw bagasse parenchyma (1500× magnification); (b) bagasse parenchyma treated by ozone for 4 h (1500× magnification); (c) raw bagasse epidermis (1500× magnification); (d) bagasse epidermis treated by ozone for 4 h (1500× magnification).

vibrations of the C−O−C linkages in ethers and esters or to phenolic hydroxyls.[38] In this work, a band representative of these functional groups was detected at 1240 cm^{-1}, which is characteristic of softwood lignins, i.e., guaiacyl type. This band was detected by Hergert after studying the infrared spectra of lignin model compounds.[32] Aromatic C−H in-plane deformation and C═O unconjugated stretching is responsible for the 1030 cm^{-1} very strong absorption band according to refs 34 and 39. A weak and well-isolated band is at 830 cm^{-1}. This band is caused by deformation vibrations of C−H out-of-plane bonds on the aromatic ring.[33]

In Figure 11, the absence of bands 1240 cm^{-1} (phenolic hydroxyl structure), 1510 cm^{-1} (phenyl-ring structure), and 1732 cm^{-1} (carbonyl group) at 4 h of ozonation could explain in particular the increasing of HCOOH and CO_2 concentrations observed by mass spectrometry at about 3−4 h of treatment (see Figure 7). The formation of these two radicals are the consequence of aromatic structure degradation to low molecular weight compounds during the ozonation process (see, e.g., Figure 3), i.e., the more they were produced, the more the rings were disrupted, reflecting the bands diminishing in FTIR spectrum. Moreover, the band structure reduction in Figure 11 somehow reflected the behavior of the chemicals plotted in Figure 9b,c, most of which are related to carbonyl groups and the low weight of aromatic rings as well, since it was possible to note that all of them were no more detected by mass spectrometry after 4 h of treatment, except for CO_2, whose reason was not explored in this paper.

Finally, in order to show the changes that occurred on the morphology of bagasse surface as a consequence of ozone interaction with biomass as a whole, Figure 12a−d illustrates SEM images of a bagasse surface before and after the ozonation procedure. From Figure 12a it could be observed that raw (or *in natura*) bagasse parenchyma shows a bundle and homogeneous structure, while the bagasse parenchyma tissue treated for 4 h has started to disrupt its surface (see Figure 12b). Moreover, in Figure 12c, one can see the epidermis of the raw material, which is composed by stomata, which are responsible for controlling the moisture content in a plant. From Figure 12c it is possible to observe some rough structures. After 4 h of ozonation, that rugosity was reduced in comparison with the raw bagasse, smoothing the epidermis surface (see Figure 12b). All these results were an indication that the ozone has really attacked the bagasse surface promoting its oxidation.

■ CONCLUSION

Mass spectrometry measurements were employed to study the interaction of ozone with sugar cane bagasse. The aim was to remove lignin prior to bagasse hydrolysis, exposing the lignocellulosic matrix to the additional enzymatic attack. The reaction mechanisms proposed in the literature are sometimes controversial. In this study, the yields of more important radicals were recorded by mass spectrometry where three phases could be observed during the treatment. The first one was characterized by the presence of CO molecule. During the second phase, radicals such as O_2, CH_3OH, OH, and H_2O appeared. Further experiments should be done to discriminated O_2 and CH_3OH since they have the same mass. The third stage was characterized by the removal of these radicals and the

dx.doi.org/10.1021/jp3121879 | J. Phys. Chem. B 2013, 117, 3110−3119

arising of the HCOOH, $CO_{,2}$ and H_3O radicals. All these results have supported Criegee's mechanism in the explanation of ozone attack of the lignin.

Physicochemical analyses have shown that the lignin content was reduced as a function of ozonation time, achieving the maximum delignification efficiency of about 65% during 4 h of treatment.

Through optical spectroscopy, the influence of typical bagasse sizes and of moisture content in bagasse during the ozonation was investigated. The results have indicated that the best condition for the ozone diffusion in the lignocellulosic matrix was for particle bagasse sizes equal to or less than 0.5 mm with wetness of 50%. This last result related to moisture content effect was in agreement with that obtained via mass spectrometry, corroborating the consistency of both techniques employed.

FTIR studies revealed that several lignin bonds were strongly affected by the ozonolysis process, giving support for the mass detection results related to Criegee's mechanism as well. The SEM technique demonstrated an alteration of the rugosity of the bagasse surface morphology after the ozonation pretreatment procedure. In conclusion, the collective results obtained from several analytical methodologies have strongly indicated that oxidative delignification of sugar cane bagasse via ozone has great potential for applications in biomass pretreatment methods, in particular for sugar cane bagasse.

AUTHOR INFORMATION

Corresponding Author

*E-mail address: jayr.amorim@gmail.com.

Notes

The authors declare no competing financial interest.

ACKNOWLEDGMENTS

The authors gratefully acknowledge FAPESP (Contract Number 2008/58034-0) for the partial financial support. The authors are grateful to Yolanda Aranda-Gonzalvo and Bertrand Retail for discussions and assistance given during the operation of the HPR60-500 system. We appreciate the technical support for FTIR and chemical analyses given by K. Marabezi and T. Pereira. Finally, the authors would like to thank the CNPEM/LNNANO/LME for collaboration during the electron microscopy work.

REFERENCES

(1) Zakzeski, J.; Bruijnincx, P. C. A.; Jongerius, A. L.; Weckhuysen, B. M. The Catalytic Valorization of Lignin for the Production of Renewable Chemicals. *Chem. Rev.* **2010**, *110*, 3552−3599.

(2) Sun, Y.; Cheng, J. Hydrolysis of Lignocellulosic Materials for Ethanol Production: A Review. *Bioresour. Technol.* **2002**, *83*, 1−11.

(3) Mosier, N.; Wyman, C.; Dale, B.; Elander, R.; Lee, Y. Y.; Holtzapple, M.; Ladisch, M. Features of Promising Technologies for Pretreatment of Lignocellulosic Biomass. *Bioresour. Technol.* **2005**, *96*, 673−686.

(4) Kumar, P.; Barrett, D. M.; Delwiche, M. J.; Stroeve, P. Methods for Pretreatment of Lignocellulosic Biomass for Efficient Hydrolysis and Biofuel Production. *Ind. Eng. Chem. Res.* **2009**, *48*, 3713−3729.

(5) Crestini, C.; D'Auria, M. Photodegradation of Lignin: The Role of Singlet Oxygen. *J. Photochem. Photobiol., A* **1996**, *101*, 69−73.

(6) Crestini, C.; D'Auria, M. Singlet Oxygen in the Photodegradation of Lignin Models. *Tetrahedron* **1997**, *53*, 7877−7888.

(7) Bonini, C.; Auria, M. D'; D' Alessio, L.; Mauriello, G.; Tofani, D.; Viggiana, D.; Zimbardi, F. Singlet Oxygen Degradation of Lignin. *J. Photochem. Photobiol., A* **1998**, *113*, 119−124.

(8) Sarkanen, K. V.; Islam, A.; Anderson, C. D. In *Methods in Lignin Chemistry*; Lin, S. Y., Dance, C. W., Eds.; Springer-Verlag: Berlin, 1992; pp 387−406.

(9) Binder, A.; Pelloni, L.; Fiechter, A. Delignification of Straw with Ozone to Enhance Biodegradability. *Eur. J. Appl. Microbiol. Biotechnol.* **1980**, *11*, 1−5.

(10) Mbachu, R. A. D.; Manley, R.; St, J. Degradation of Lignin by Ozone I: The Kinetics of Lignin Degradation of Ozone. *J. Polym. Sci., Polym. Chem.* **1981**, *19*, 2053−2063.

(11) Vidal, P. F.; Molinier, J. Ozonolysis of Lignin: Improvement of *in vitro* Digestibility of Poplar Sawdust. *Biomass* **1988**, *16*, 1−17.

(12) Kwon, J.-Y.; Chung, P.-G.; Lim, I.-H. Removal of Residual COD in Biologically Treated Paper-Mill Effluent and Degradation of Lignin Using Nonthermal Plasma Unit. *J. Environ. Sci. Health, Part A* **2004**, *39*, 1853−1865.

(13) Schultz-Jensen, N.; Leipold, F.; Bindslev, H.; Thomsen, A. B. Plasma-Assisted Pretreatment of Wheat Straw. *Appl. Biochem. Biotechnol.* **2011**, *163*, 558−572.

(14) Schultz-Jensen, N.; Kádár, Z.; Thomsen, A. B.; Bindslev, H.; Leipold, F. Plasma-Assisted Pretreatment of Wheat Straw for Ethanol Production. *Appl. Biochem. Biotechnol.* **2011**, *165*, 1010−1023.

(15) Bailey, P. S. *Ozonation in Organic Chemistry: Olefinic Compounds*; Academic Press: New York, 1978, Vol. *1*.

(16) Eriksson, T.; Gierer, J. Studies on the Ozonation of Structural Elements in Residual Kraft Lignins. *J. Wood Chem. Technol.* **1985**, *5*, 53−84.

(17) Heitner, C.; Dimmel, D.; Schmidt, J. A. *Lignin and Lignans: Advances in Chemistry*; Taylor & Francis Group: Boca Raton, FL, 2010.

(18) Criegee, R. Mechanism of Ozonolysis. *Angew. Chem., Int. Ed.* **1975**, *14*, 745−751.

(19) Nascimento, E. A.; Morais, S. A. L.; Aquino, F. J. T.; Piló-Veloso, D. Ozonólise das Ligninas Organossolve e Kraft Eucalipto. Parte II: Cinética nos Meios Ácido e Básico. *Quím. Nova* **1998**, *21*, 578−583.

(20) Bentley, K. W. In *Techniques of Organic Chemistry Part 2*; Weissberger, A., Ed.; Wiley-Interscience: New York, 1963; Vol. *XI*, pp 875−906.

(21) Bailey, P. In *Ozone Chemistry and Technology*; Murphy, J. S., Orr, J. R., Eds.; The Franklin Institute Press: Philadelphia, PA, 1975; pp 77−83.

(22) Ragnar, M. On the Importance of Radical Formation in Ozone Bleaching, Ph.D. Thesis, Royal Institute of Technology, Department of Pulp and Paper Technology, Department of Wood Chemistry, Stockholm, Sweden, 2000.

(23) Saito, K.; Kato, T.; Tsuji, Y.; Fukushima, K. Identifying the Characteristic Secondary Ions of Lignin Polymer Using ToF-SIMS. *Biomacromolecules* **2005**, *6*, 678−683.

(24) Saito, K.; Kato, T.; Takamori, H.; Kishimoto, T.; Yamamoto, A.; Fukushima, K. A New Analysis of the Depolymerized Fragments of Lignin Polymer in the Plant Cell Walls Using ToF-SIMS. *Appl. Surf. Sci.* **2006**, *252*, 6734−6737.

(25) Saito, K.; Kishimoto, T.; Matsushita, Y.; Imaia, T.; Fukushima, K. Application of TOF-SIMS to the Direct Determination of Syringyl to Guaiacyl (S/G) Ratio of Lignin. *Surf. Interface Anal.* **2011**, *43*, 281−284.

(26) Morreel, K.; Dima, O.; Kim, H.; Lu, F.; Niculaes, C.; Vanholme, R.; Dauwe, R.; Goeminne, G.; Inzé, D.; Messens, E.; Ralph, J.; Boerjan, W. Mass Spectrometry-Based Sequencing of Lignin Oligomers. *Plant. Physiol.* **2010**, *153*, 1464−1478.

(27) Saito, K.; Watanabe, Y.; Shirakawa, M.; Matsushita, Y.; Imai, T.; Koike, T.; Sano, Y.; Funada, R.; Fukazawa, K.; Fukushima, K. Direct Mapping of Morphological Distribution of Syringyl and Guaiacyl Lignin in the Xylem of Maple by Time-of-Flight Secondary Ion Mass Spectrometry. *Plant J.* **2012**, *69*, 542−552.

(28) *EQP/EQS Analyzer Operator's Manual*, Doc. No HA-111-675; Hiden Analytical: Warrington, U.K., 2007.

(29) Orphal, J. A Critical Review of the Absorption Cross-Sections of O_3 and NO_2 in the Ultraviolet and Visible. *J. Photochem. Photobiol. A* **2003**, *157*, 185−209.

(30) Rocha, G. J. M.; Silva, F. T.; Araújo, G. T.; Curvelo, A. A. S. In *Proceedings of the Fifth Brazilian Symposium on the Chemistry of Lignin and Other Wood Components*; Sépia Ed.a e Gráfica: Curitiba, Brazil, 1997; pp 113−115.
(31) Gouveia, E. R.; Nascimento, R. T.; Souto-Maior, A. M.; Rocha, G. J. M. Validation of the Methodology for the Chemical Characterization of the Sugarcane Bagasse. *Quím. Nova* **2009**, *32*, 1500−1503.
(32) Hergert, H. L. Infrared Spectra of Lignin and Related Compounds. II. Conifer Lignin and Model Compounds. *J. Org. Chem.* **1960**, *25*, 405−413.
(33) Lina, S. Y.; Dence, C. W., Eds. *Methods in Lignin Chemistry*; Springer-Verlag: New York, 1992.
(34) Schwanninger, M.; Rodrigues, J. C.; Pereira, H.; Hinterstoisser, B. Effects of Short-Time Vibratory Ball Milling on the Shape of FT-IR Spectra of Wood and Cellulose. *Vib. Spectrosc.* **2004**, *36*, 23−40.
(35) Yu, P. Molecular Chemistry Imaging to Reveal Structural Features of Various Plant Feed Tissues. *J. Struct. Biol.* **2005**, *150*, 81−89.
(36) Schultz, H.; Baranska, M. Identification and Quantification of Valuable Substances by IR and Raman Spectroscopy. *Vib. Spectrosc.* **2007**, *43*, 13−25.
(37) Sun, X. F.; Xu, F.; Sun, R. C.; Fowler, P.; Baird, M. S. Characteristics of Degraded Cellulose Obtained from Steam-Exploded Wheat Straw. *Carbohydr. Res.* **2005**, *340*, 97−106.
(38) Fengel, D.; Ludwig, M. Möglichkeiten und Grenzen der FTIR-Spektroskopie bei der Charakterisierung von Cellulose. *Das Papier* **1991**, *45*, 45−51.
(39) Popescu, C.-M.; Popescu, M.-C.; Singurel, G.; Vasile, C.; Argyropolus, D. S.; Willfor, S. Spectral Characterization of Eucalyptus Wood. *Appl. Spectrosc.* **2007**, *61*, 1168−1177.